

Design of efficient lens ducts

Rulian Fu, Guangjun Wang, Zhaoqi Wang, Enxu Ba, Guoguang Mu, and Xin-Hua Hu

Lens ducts have the potential to couple the output from a laser diode array efficiently into the gain medium of a solid-state laser in an end-pumped configuration. Using a ray-tracing method we investigate different design approaches of lens ducts and demonstrate the possibility to obtain an output beam with a symmetric profile that is insensitive to the small displacement from the output surface of a lens duct. © 1998 Optical Society of America

OCIS codes: 140.3300, 140.3580, 220.2740, 220.0220.

1. Introduction

All-solid-state lasers with laser diodes as pumping sources have attracted a large research and development effort in recent years because of their potential to achieve high reliability and energy efficiency. Among these lasers, an end-pumped configuration is preferred whenever the requirements of high efficiency and good mode structure inside the cavity are necessary. However, the highly divergent output from a laser diode array presents a great challenge to researchers in search of highly efficient and yet simple optical devices that can couple the output from a laser diode array into a gain medium. A nonimaging lens duct has emerged in the past few years as a promising candidate to meet these challenges.^{1,2} Together with a cylindrical microlens, which reduces the divergence angle of the laser diode from approximately 40° to less than 3° in the fast-axis direction, the use of a lens duct can significantly increase the irradiance from a laser diode array on a gain medium in the end-pumped configuration. In comparison with other coupling methods such as gradient-index lenses,³ optical fibers,⁴ aspheric lenses⁵ or direct coupling,⁶ the lens duct has the advantages of high coupling efficiency, simple structure, and insensitivity to minor misalignment. These advantages are especially important for the design of high power lasers with large laser diode arrays as the pump source. In

contrast, the monolithic lens duct is a nonimaging light collection device that cannot be characterized by simple geometrical-optics formulas. The difficulty of analysis can impede the wide application of this device in all-solid-state lasers.

Here we report the investigation of lens ducts based on the conventional ray-tracing method. Different approaches are compared to determine an efficient design of the lens duct. Preliminary experimental results of lens duct coupling is obtained from a Nd:YAG laser end pumped with a high power quasi-cw laser diode array.

2. Ray-Tracing Calculation

A lens duct is a glass device that can consist of one spherical input surface and five planar surfaces. The spherical surface is designed for efficient collection of the output radiation from a laser diode array into the duct. As the light rays proceed into the duct, they are incident on one of the four canted side surfaces and, ideally, are totally reflected from the side surfaces until they reach the planar output surface opposite the input surface. Once transmitted through the output surface with dimensions that match the center area of a gain medium, the light rays are injected into the gain medium with little loss because of the proximity of the output surface to the gain medium. The objectives of lens duct design are high coupling efficiency and high quality profile of the output beam for pumping, which is related directly to the mode structure of the beam inside the laser cavity. These objectives can be achieved through careful selection of the lens duct parameters to reduce the reflection loss at side surfaces and to adapt to the specific dimensions of the laser diode array and gain medium.

We designed lens ducts using the conventional ray-tracing method. A two-dimensional schematic of a

R. Fu, G. Wang, Z. Wang, E. Ba, and G. Mu are with the Institute of Modern Optics, Nankai University, Tianjin 300071, China. X.-H. Hu is with the Department of Physics, East Carolina University, Greenville, North Carolina 27858.

Received 14 October 1997; revised manuscript received 17 February 1998.

0003-6935/98/184000-04\$15.00/0

© 1998 Optical Society of America

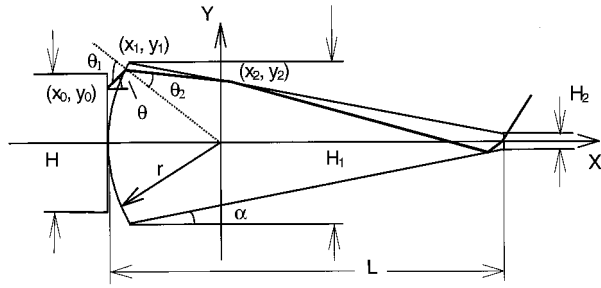


Fig. 1. Schematic of a lens duct in the slow-axis plane of the laser diode in which r is the radius of the spherical input surface, L is the length of the duct, and H_1 and H_2 are the widths of the input and output surfaces, respectively.

lens duct with four key parameters, r , L , H_1 , and H_2 , defined in the x - y plane or the slow-axis plane of the laser diode is shown in Fig. 1. Parameter r is the radius of the input surface, L is the length of the duct, H_1 is the width of the input surface, and H_2 is the width of the output surface. For our calculations we assumed that the output surface is square and thus H_3 , the width of the output surface in the x - z plane or the fast-axis plane, is equal to H_2 .

The focal length of the spherical input surface is given by $f = rn/(n - 1)$, where n is the refractive index of the glass at the pump light wavelength. Using a coordinate system with its origin overlapping the center of the spherical input surface, we considered a general light ray that originates from a point (x_0, y_0) on surface H , which could be the front surface of a laser diode or a microlens bar. Without loss of generality, we assumed that $y_0 > 0$ and the ray forms an angle θ with respect to the x axis. The point (x_1, y_1) at which the ray is incident on the input surface of the lens duct is determined by

$$y_1 - y_0 = (x_1 - x_0)\tan \theta, \quad (1)$$

$$x_1^2 + y_1^2 = r^2. \quad (2)$$

The refractive angle of ray θ_2 can be found by use of Snell's law:

$$n \sin \theta_2 = \sin \theta_1, \quad (3)$$

where incident angle $\theta_1 = \theta + \arcsin(y_1/r)$. Furthermore, the intersecting point (x_2, y_2) of the refracted ray with a canted side surface can be related to the lens duct parameters (r, L, H_1, H_2) by the following equations:

$$y_2 - y_1 = (x_2 - x_1)\tan[\theta_2 - \arcsin(y_1/r)], \quad (4)$$

$$\frac{y_2 - H_1/2}{x_2 + \sqrt{r^2 - (H_1/2)^2}} = \frac{(H_1 - H_2)/2}{-\sqrt{r^2 - (H_1/2)^2} - (L - r)}. \quad (5)$$

The considered ray is reflected from the side surface at (x_2, y_2) with an angle θ_3 with respect to the x axis given by

$$\theta_3 = -[\theta_2 - \arcsin(y_1/r)] - 2\alpha, \quad (6)$$

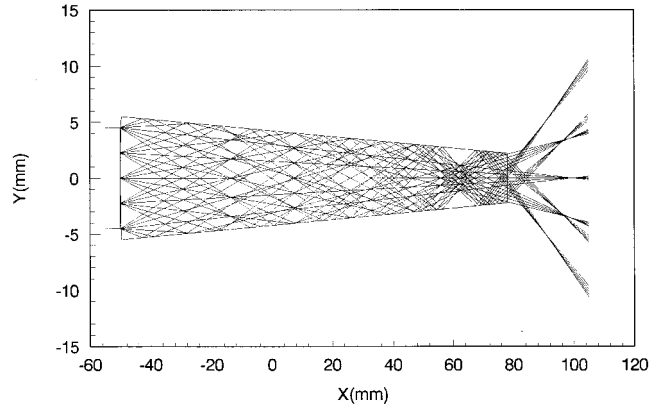


Fig. 2. Example of ray tracing inside a lens duct with H as the width of the originating surface of the pump beam from a laser diode array with $H = 9$ mm, $r = 50$ mm, $H_1 = 11$ mm, and $H_2 = 4.5$ mm.

where α is the inclination angle of the side surface with respect to the x axis, satisfying

$$\sin \alpha = \frac{H_1 - H_2}{2(L - r) + \sqrt{4r^2 - H_1^2}}. \quad (7)$$

If the ray reflects further from side surfaces, the next intersecting point can be calculated from the following two equations:

$$y_3 - y_2 = (x_3 - x_2)\tan \theta_3, \quad (8)$$

$$\frac{y_3 + H_1/2}{x_3 + \sqrt{r^2 - (H_1/2)^2}} = \frac{(H_2 - H_1)/2}{\sqrt{r^2 - (H_1/2)^2} - (L - r)}. \quad (9)$$

Using Eqs. (4)–(9) we calculated the propagation of various rays in a lens duct. For the following results we considered a quasi-cw laser diode array consisting of five 10-mm-long diode bars stacked on top of each other. The center-to-center distance between adjacent bars is 0.5 mm. Thus, the array has a dimension of 10 mm in the slow-axis direction and 2 mm in the fast-axis direction. The output of the laser diode array is reshaped by a microlens array, reducing the divergence angle in the fast-axis plane from 40° to approximately 3° , whereas the angle in the slow-axis plane remains at 10° . The distance between the microlens array surface and the apex of the input surface of the lens duct was assumed to be 0.1 mm.

A typical result of ray tracing in the slow-axis plane or the x - y plane is shown in Fig. 2. Note that the irradiance of the radiation inside the lens duct is far from homogeneous. Moreover, the inside distribution of the irradiance and consequently that directly outside the output surface of the lens duct can be favorably varied with different lens duct parameters. We illustrate this aspect of the lens duct design with two different approaches.

A. Single-Reflection Approach

For the single-reflection approach the lens duct was designed to have all the light rays reflected from one

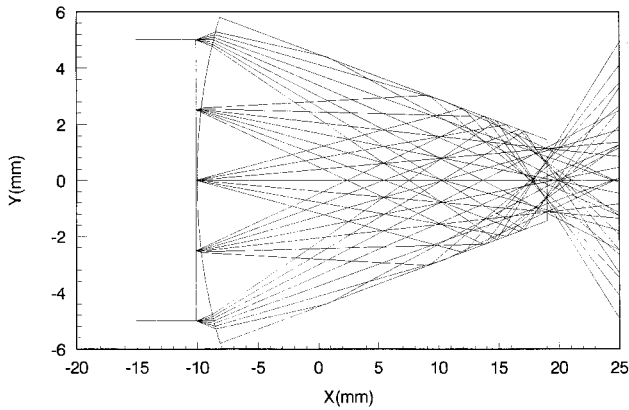


Fig. 3. Ray-tracing result from the single-reflection approach for a lens duct with $H = 10$ mm, $r = 10$ mm, $H_1 = 11.6$ mm, $H_2 = 2.9$ mm, and $L = 28$ mm.

side surface only after the rays were inside the duct and before they exited through the output surface. Consequently, the length of the lens duct is fairly small, which has the advantages of reduced loss and a compact size. The corresponding ray-tracing result in the slow-axis plane is shown in Fig. 3. Within each bundle, the most diverging rays converge to the center area of the output surface of the duct. The corresponding distribution of the normalized irradiance outside the output surface is plotted as a function of y/H_2 in Fig. 4. A top-hat distribution is obtained precisely at the output surface. The spatial profile of the output beam spreads out and becomes smooth as the distance from output surface d increases. For $d > 1$ mm the beam profiles have a form close to a Gaussian distribution, which may be necessary for mode matching inside the cavity of the pumped laser.

B. Converging Approach

As shown in Fig. 2, the light rays can be concentrated in a small area after several reflections from the side surfaces, indicating the possibility of creating a beam

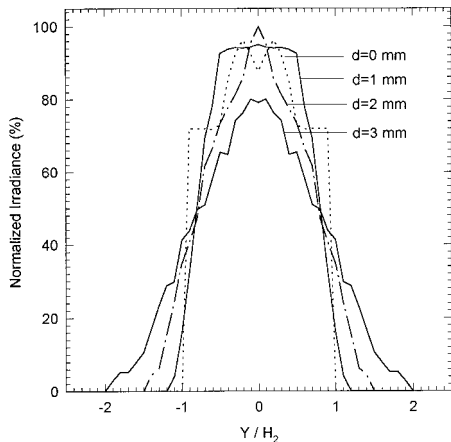


Fig. 4. Normalized irradiance distribution of the same lens duct as in Fig. 3 except in the slow-axis direction.

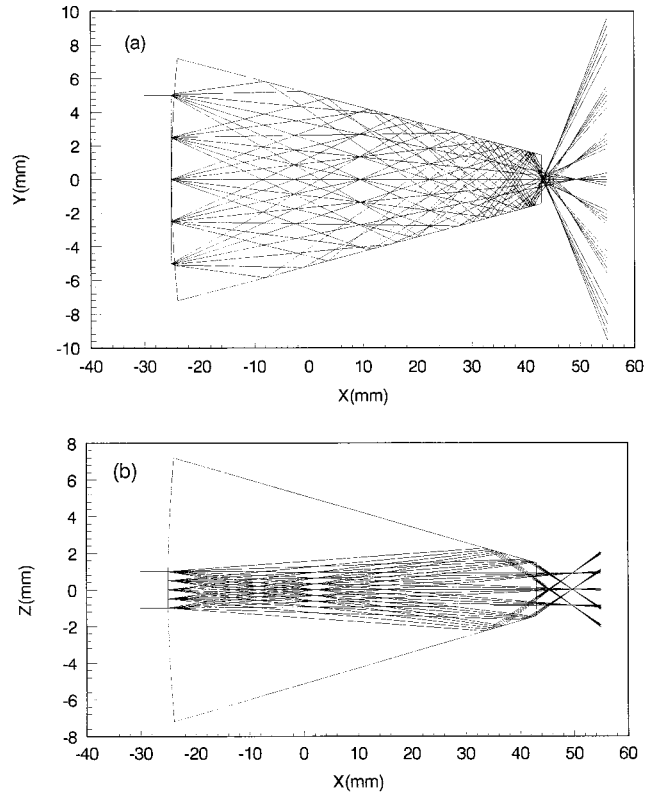


Fig. 5. Ray-tracing results of a lens duct from the converging approach in (a) the slow-axis plane assuming 10° for the divergence angle of the incoming ray bundles and (b) in the fast-axis plane with a 3° divergence angle with $H = 10$ mm, $r = 25$ mm, $H_1 = 14.4$ mm, $H_2 = 2.9$ mm, and $L = 68$ mm.

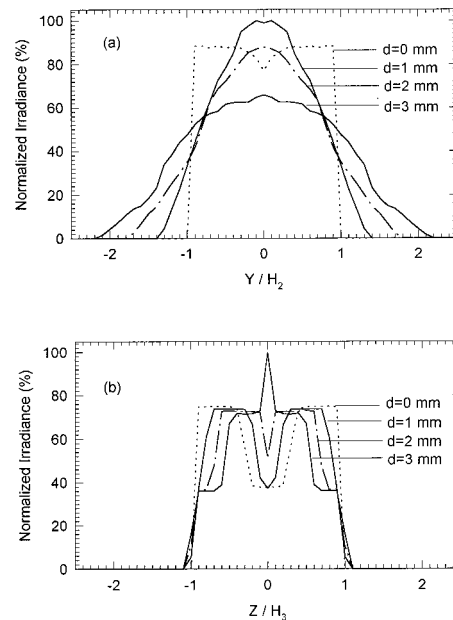


Fig. 6. Normalized irradiance distribution of the same lens duct as in Fig. 5: (a) in the slow-axis direction with a 10° divergence angle and (b) in the fast-axis direction with a 3° divergence angle.

of high irradiance. In this approach the radius of the input surface and the duct length increase from the single-reflection approach so that the output surface is located near the area in which the rays are concentrated. Figure 5 displays the ray-tracing results of this approach in both the slow-axis and fast-axis planes whereas the corresponding irradiance distributions are plotted in Fig. 6, where $H_3 (=H_2)$ is the width of the lens duct in the fast-axis direction. From these results one can see that the profiles of the output beam in the slow-axis direction are close to a Gaussian distribution and not sensitive to distance d . In contrast, the output beam profile is much more irregular in the fast-axis direction than that in the slow-axis direction. We found, however, that, if the divergence angle in the fast-axis direction was increased from 3° to 10° , the same as in the slow-axis direction, the beam profiles became smooth as shown in Fig. 7. Therefore, it is possible to obtain a symmetric profile in the transverse y - z plane for the output beam from the lens duct that is close to a two-dimensional Gaussian distribution if the divergence angles of the laser diode beams can be controlled to be about the same by a suitable microlens.

3. Discussion

We have calculated the beam profiles of the lens duct output based on ray tracing in the slow-axis and the fast-axis directions to demonstrate that a smooth and symmetric beam can be obtained for solid-state laser pumping with high power laser diode arrays. Based on this analysis we fabricated several lens ducts using the converging approach design. Coupling efficiency as high as 87% was obtained for lens ducts with no antireflection coatings using the quasi-cw laser diode array described above.

This project is supported by a research grant from the National Commission of Science and Technology of China and a travel grant to X.-H. Hu from the East Carolina University, Greenville, N.C.

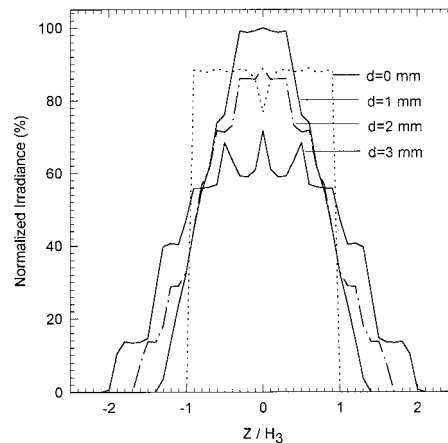


Fig. 7. Normalized irradiance distribution of the same lens duct as in Fig. 5 except in the fast-axis direction with a 10° divergence angle.

All correspondence and reprint requests should be sent to X.-H. Hu, Department of Physics, East Carolina University, Greenville, N.C. 27858.

References

1. R. J. Beach, "Theory and optimization of lens ducts," *Appl. Opt.* **35**, 2005–2015 (1996).
2. G. Feugnet, C. Bussac, C. Larat, and M. Schwarz, "High efficiency TEM₀₀ Nd:YVO₄ laser longitudinally pumped by a high-power array," *Opt. Lett.* **20**, 157–159 (1995).
3. B. Zhou, T. J. Kane, G. J. Dixon, and R. L. Byer, "Efficient, frequency-stable laser-diode-pumped Nd:YLF laser," *Opt. Lett.* **10**, 62–64 (1985).
4. Th. Graf and J. E. Balmer, "High power Nd:YLF laser end pumped by a diode-laser bar," *Opt. Lett.* **18**, 1317–1319 (1993).
5. L. Turi and T. Juhasz, "High-power longitudinal end-diode-pumped Nd:YLF regenerative amplifier," *Opt. Lett.* **20**, 154–156 (1995).
6. T. Taira and T. Kobayshi, "Intracavity frequency doubling and Q-switching in diode-laser-pumped Nd:YVO₄ lasers," *Appl. Opt.* **34**, 4298–4301 (1995).